Effect of Filler Content and Size on the Properties of Ethylene Vinyl Acetate Copolymer–Wood Fiber Composites

D. G. Dikobe, A. S. Luyt

Department of Chemistry, University of the Free State (Qwaqwa Campus), Private Bag X13, Phuthaditjhaba 9866, South Africa

Received 27 June 2006; accepted 4 September 2006
DOI 10.1002/app.25513
Published online in Wiley InterScience (www.interscience.wiley.com).

ABSTRACT: In this study, the main focus was on the effect of wood fiber (WF) content and particle size on the morphology and mechanical, thermal, and water-absorption properties of uncompatibilized and ethylene glycidyl methacrylate copolymer (EGMA) compatibilized ethylene vinyl acetate copolymer–WF composites. For uncompatibilized composites, the tensile strength decreased with increasing WF content, whereas for compatibilized composites, the tensile strength initially decreased, but it increased for composites containing more than 5% WF. Small-WF-particle-containing composites had higher tensile strengths than composites containing larger WF particles, both in the presence and absence of EGMA. WF particle size did not seem to have much influence on the degradation behavior of the composites, whereas water absorption by the composites seemed to be higher in composites with smaller particle sizes for both compatibilized and uncompatibilized composites. © 2006 Wiley Periodicals, Inc. J Appl Polym Sci 103: 3645–3654, 2007

Key words: composites; mechanical properties; renewable resources, structure-property relations; thermal properties

INTRODUCTION

The use of lignocellulosic materials, especially wood, as fillers in polymer composites has appeared to gain popularity and importance, particularly because of the low cost of wood and the increase in applications of the resulting wood–polymer composites. The increase in applications has been due to the fact that the resulting wood fiber (WF)–polymer composites usually have high specific mechanical properties that the two constituents do not have individually.[1,2] Because the mechanical properties of heterogeneous structures depend on the quality of interfaces between the components, it is crucial to develop additive substances favoring chemical bonds (compatibilizer) between the natural fiber and the matrix. The reasons natural fibers do not perform satisfactorily as polymer reinforcers are their high percentage of hydroxyl groups and high surface polarities.[1,3–6] In a composite, the efficiency of the filler depends primarily on its ability to transfer the applied stress from the continuous phase (matrix) to the fibers. This is not achieved with WFs because of poor adhesion between the hydrophilic surface of the natural fibers and the essentially hydrophobic polymers that are commonly used as the matrix.[1,7,8] Different chemical substances have been used as compatibilizers of wood–polymer composites by various researchers.[3,9,10] To improve the compatibility between WFs and linear low-density polyethylene (LDPE) matrix, Liao et al.[11] treated WFs with titanate coupling agents or grafting by acrylonitrile. Both treatments resulted in an improvement in the mechanical properties of the resultant composites compared with composites filled with untreated WFs. Malunka et al.[10] investigated uncrosslinked and crosslinked ethylene vinyl acetate copolymer (EVA)–sisal fiber composites and reported dicumyl peroxide (DCP) to be effective in grafting EVA to sisal fiber; this resulted in composites with better properties than uncrosslinked composites. Sedlackova et al.[12] reported the ability of poly(ethylene-*co*-methacrylic acid) copolymer (EMAA) to effectively compatibilize a LDPE–WF composite. Both mechanical and dynamic mechanical results showed that EMAA promoted better interaction between LDPE and WF. The mechanical properties of compression-molded polystyrenes filled with the sawdust wood residue of softwood and hardwood species were investigated by Maldas et al.[6] To improve the compatibility of the WFs with the polymer matrices, different treatments (e.g., graft copolymerization) and coupling agents (e.g., silanes and isocyanates at various concentrations) were used. The mechanical properties were considerably improved in the treated polystyrene–WF composites compared to the untreated

Correspondence to: A. S. Luyt (luytas@qwa.uovs.ac.za).
Contract grant sponsor: National Research Foundation in South Africa; contract grant number: GUN 2050677.
Contract grant sponsor: University of the Free State.

Journal of Applied Polymer Science, Vol. 103, 3645–3654 (2007)

ones. The compatibilizing agents became chemically linked to the hydrophilic WFs and facilitate the wetting of the hydrophobic polymer chains. Compatibilizers should, therefore, have both hydrophobic and hydrophilic characteristics, which makes bonding between the two constituents much easier.

Other factors that influence the properties of WF composites are the content and particle sizes of the fibers used. Sedlackova et al.[12] reported that a high content of WF and a low content of EMAA in their system yielded materials with high moduli and high tensile strengths. Zaini et al.[13] reported the effect of filler content and size on the mechanical properties of propylene–oil palm WF composites; they reported that the composite filled with larger sized filler showed a higher modulus and tensile and impact strengths, particularly at higher filler loadings. Ismail et al.[14] studied the effect of filler content and size on oil palm–WF reinforced epoxidized natural rubber composites and reported that the tensile strength of the composites decreased with an increase in filler content because of the inability of the filler to support stress transferred from the polymer matrix. It was also reported that the filler with a smaller particle size exhibited a higher tensile strength than fillers with a larger particle size because of better filler dispersion and filler–matrix interaction.

In this study, the effect of WF size and content on the morphology and mechanical, thermal, and water absorption properties of uncompatibilized and 10% ethylene glycidyl methacrylate copolymer (EGMA) compatibilized EVA–WF composites were investigated.

EXPERIMENTAL

EVA with a 9% vinyl acetate content was used as composite matrix. It had a density of 0.93 g/cm^3, a melting point of 95°C, a tensile strength of 19 MPa, and an elongation at break of 750%. EGMA was used as compatibilizer. It had a density of 0.93 g/cm^3, a melting point of 93°C, a tensile strength of 12 MPa, and an elongation at break of 440%. Both polymers were supplied by Plastamid (Elsies River, South Africa).

Pine WF, or pine saw dust, was obtained from FBW Taurus (Phuthaditjhaba, South Africa). It was supplied as light orange powder with a density of 1.5 g/cm^3. We produced different WF particles sizes (<150, 151–300, and 301–600 μm) by sieving the received WF with laboratory test sieves with relevant pore sizes. The WF was in powder form with a small aspect ratio.

Samples were weighed according to the required ratios to consist of a total of 40 g (which was the mass required for thoroughly mixing the different components in the Brabender mixer, Duisburg, Germany). Mixing of the samples was done at a temperature of 130°C and a mixing speed of 30 min^{-1} for 15 min. The samples were then melt-pressed at 120°C and 100 bar for 5 min. Pressed samples were allowed to cool at room temperature for 10 min before they were handled to avoid air from penetrating, which would promote the formation of bubbles.

The morphologies of the EVA–WF composites were examined with polarized optical microscopy and scanning electron microscopy (SEM). For polarized optical microscopy analysis, a very thin film of the sample was placed on a glass slide, and polarized optical photos were taken at 100× magnification with a CETI polarized optical microscope made in Belgium. The photos were taken with a Ceist DCM digital camera. SEM analyses were done on the fracture surfaces of the samples with a Jeol 6400 WINSEM scanning electron microscope (Tokyo, Japan) at 5 keV.

Differential scanning calorimetry (DSC) analyses were carried out on a PerkinElmer DSC7 differential scanning calorimeter (Wellesley, MA) under flowing nitrogen (20 mL/min). Samples with a mass of ±7.5 mg were heated from 25 to 150°C at a rate of 20°C/min, held at 25°C for 1 min to eliminate thermal history, cooled to 25°C, and reheated under the same conditions. The melting and crystallization data were obtained from the second scan.

Thermogravimetric analysis (TGA) was carried out with a PerkinElmer TGA7 thermogravimetric analyzer. Samples of mass ±10 mg were heated from 50 to 600°C at a heating rate of 20°C/min under flowing nitrogen (20 mL/min).

Tensile properties were determined with a Hounsfield H5KS (Hounsfield Test Equipment, Redhill, England) tensile tester. At least eight dumbbell samples, with a gauge length of 24 mm, for each composite were analyzed at a speed of 50 mm/min.

For water absorption determinations, samples were cut into 30 × 20 mm sheets. They were dried at 70°C until they reached a constant weight. The samples were then immersed into a static distilled water bath at room temperature. Water uptake at time t of the composites was calculated with eq. (1):

$$\text{Water uptake } (\%) = (M_t - M_0)/M_0 \times 100 \quad (1)$$

where M_t is the mass of the sample at time t and M_0 is the mass of the sample before insertion into the water. Samples were immersed in water for 72 h, and water uptake measurements were recorded at 24-h intervals. The water uptake was plotted as a function of time.

RESULTS AND DISCUSSION

Microscopy

We observed the effect of particle size on the morphology of the EVA–WF composites by comparing the photos on the left and right in Figure 1. When

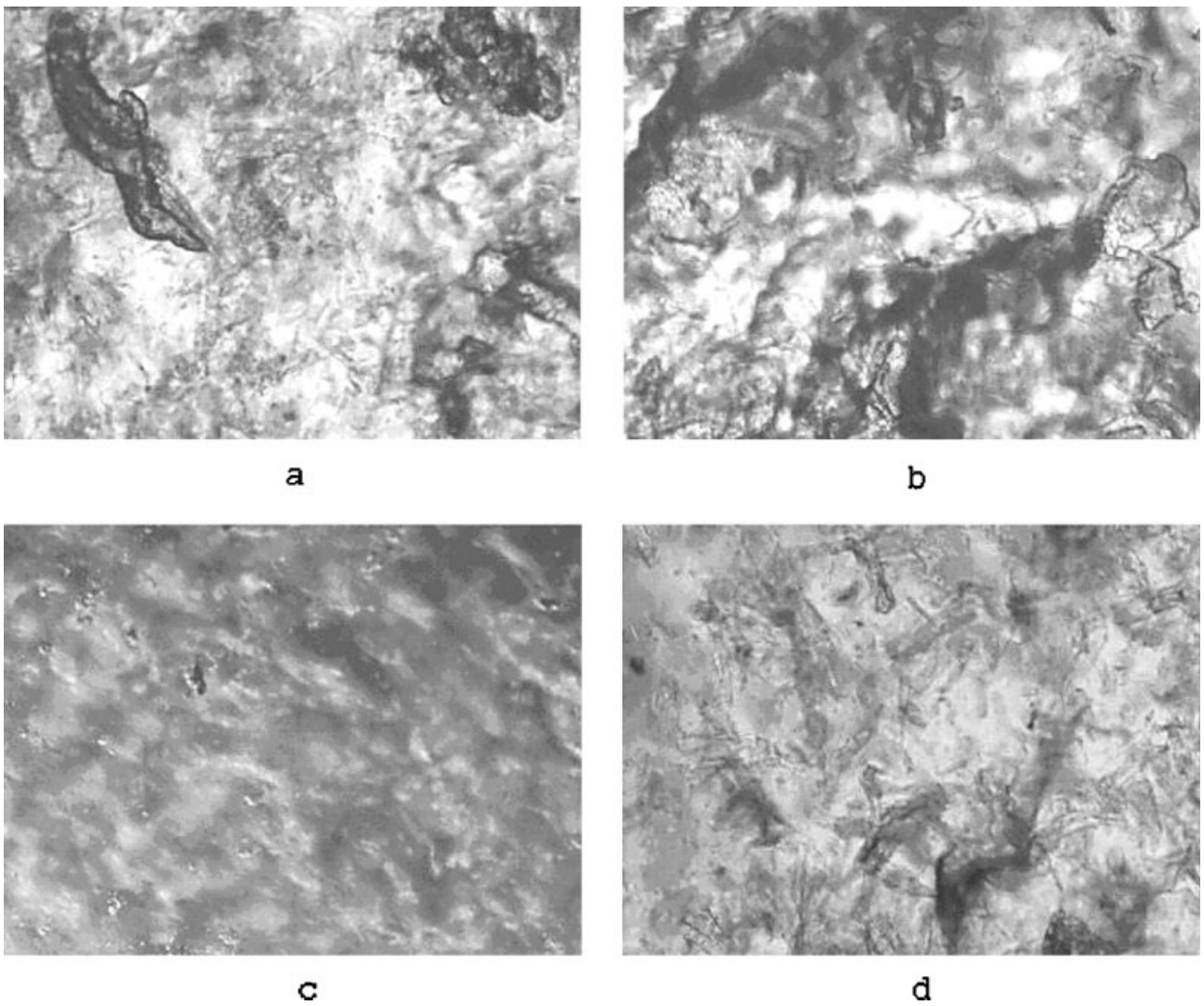

Figure 1 Polarized optical microscopy photos (100×) of the EVA–WF and EVA/EGMA–WF composites: (a) 95 : 5 w/w EVA/WF (<150 μm), (b) 95 : 5 w/w EVA/WF (301–600 μm), (c) 85 : 10 : 5 w/w EVA/EGMA/WF (<150 μm), and (d) 85 : 10 : 5 w/w EVA/EGMA/WF (301–600 μm).

5% of WF particles smaller than 150 μm and 301–600 μm particles were used in the 95 : 5 w/w EVA/WF composite, there was better compatibility between the filler and the matrix when smaller WF particles were used. A better bonding quality between the two phases was observed when smaller (<150 μm) WF particles were used compared to the larger (301–600 μm) particles. Salemane and Luyt[9] reported that the difference in WF particle size had an effect on the morphological structures of the composites. According to these authors, composites with smaller WF particles (<38 μm) had smoother surfaces than those containing larger particles (301–600 μm). In the 85 : 10 : 5 w/w EVA/EGMA/WF composites (<150 and 301–600 μm), adhesion between the two phases was improved compared to the uncompatibilized composites, but it was still evident that the particles smaller than 150 μm interacted better with the matrix than the 301–600 μm particles.

Figure 2 shows SEM photos of the uncompatibilized and 10% EGMA compatibilized composites containing 25% WF. Figure 2(a) clearly shows WF rupture on breaking the polymer sample; this indicates good interfacial adhesion between WF and the matrix. The opposite is obvious from Figure 2(b), where there are indications of fiber pullout from the matrix.

DSC

The influence of less than 150-μm WF content on the melting behavior of uncompatibilized composites is shown in Figure 3. The curves show a single endothermic peak around 95°C, the temperature at which EVA melts. The melting temperature was not influenced, within experimental error, by the WF content in the samples. There was no increasing or decreasing trend, which means that crystal thickness was

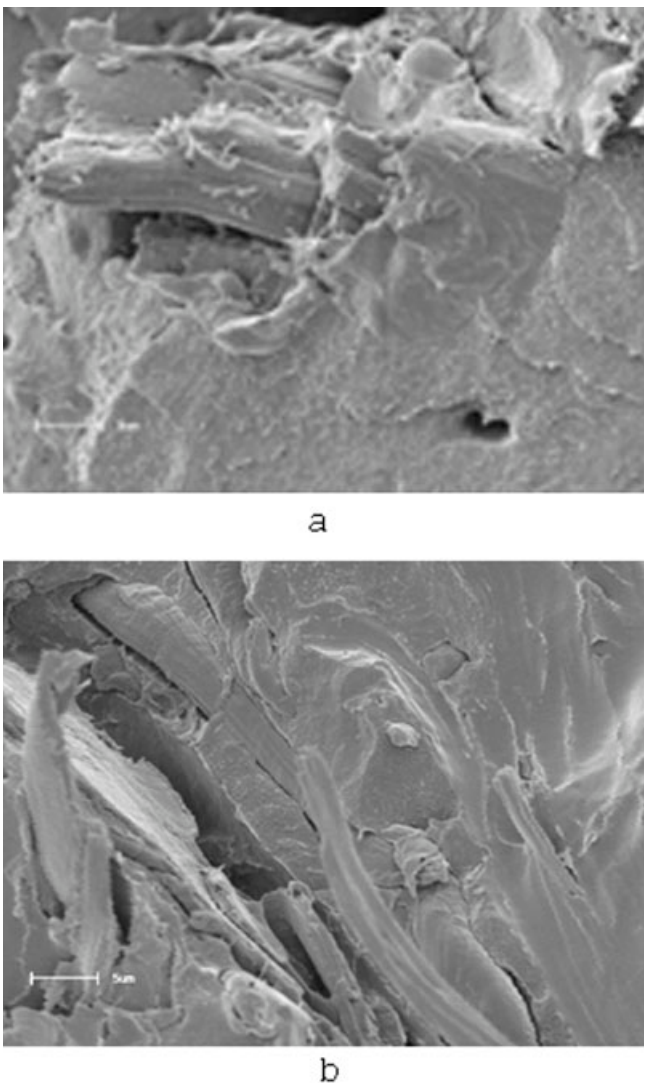

Figure 2 SEM photos (4000×) of the (a) 65 : 10 : 25 w/w EVA/EGMA/WF and (b) 75 : 25 w/w EVA/WF composites.

not influenced consistently by increasing WF content.

Pure EVA had the highest melting enthalpy (ΔH_m), and generally, there was a decrease in ΔH_m as more WF was present in the samples, which was to be expected because of the decreasing EVA/WF ratio in the samples. The theoretically expected enthalpy values ($\Delta H_m^{\text{theor}}$; with ΔH_m of pure EVA and the original EVA/WF mixing ratios taken into account) were not very different from the experimental values (ΔH_m^{exp}). $\Delta H_m^{\text{theor}}$ was calculated with the following equation:

$$\Delta H_m^{\text{theor}} = \Delta H_m^{\text{exp}} \times \text{EVA fraction in the composite}$$

The EVA part of the composite still crystallized fairly normally, even though it was clear that the crystals were not as perfect as before, as shown by the broadening of the peaks for samples containing more WF (Fig. 3). The formation of perfect crystals was hindered by the presence of the WF particles, which probably gave rise to epitaxial crystallization on the surfaces of the WF particles distributed throughout the polymer matrix.

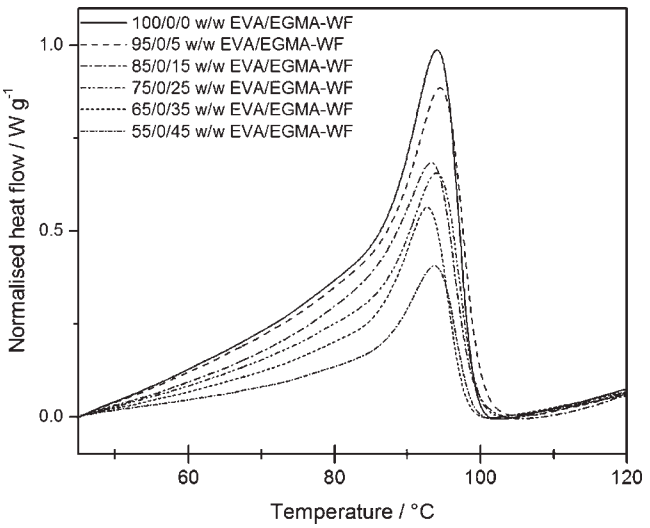

Figure 3 DSC heating curves of pure EVA and the EVA–WF (<150 μm) composites at different WF ratios.

We investigated the effect of WF particle sizes (<150, 151–300, and 301–600 μm, unsieved) by looking at the 75 : 25 w/w EVA/WF composites. Figure 4 shows the melting peaks of the composites prepared with particles smaller than 150 μm, 151–300 and 301–600 μm particles, and unsieved particles. There was a slight decrease in peak temperature of melting with increasing WF particle size, and there were obvious differences in the ΔH_m's of the samples containing WF with different particle sizes, although there was no trend. From this, it was clear that WF particle

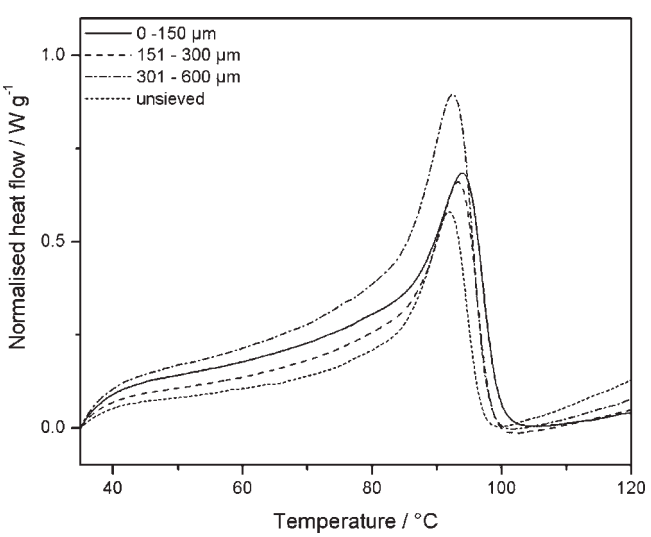

Figure 4 Effect of WF particle size on the DSC melting behavior of the 75 : 25 w/w EVA/WF composites.

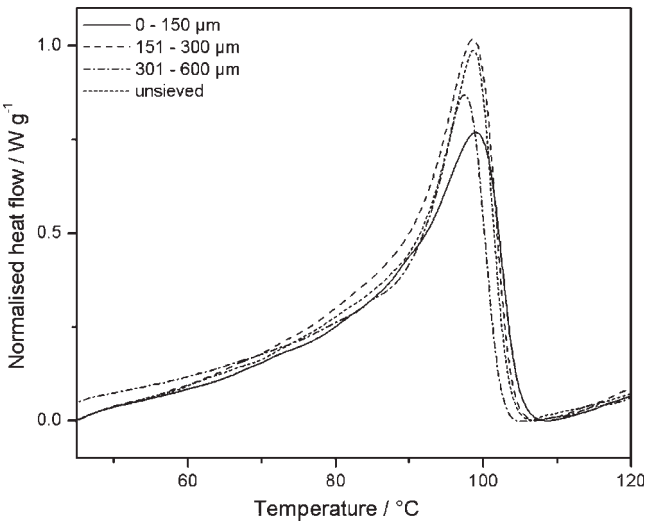

Figure 5 Effect of WF particle size on the DSC melting behavior of the 5 : 10 : 25 w/w EVA/EGMA/WF composites.

size influenced the crystallization behavior of EVA, probably through the restriction of EVA chain mobility and by WF particles acting as nuclei for epitaxial crystallization. However, differences in WF distribution in the matrix and differences in WF particle shape probably played a significant role in the crystallization behavior of EVA in the presence of WF. Figure 5 shows the effect of WF particle size on the DSC melting behavior of the 65 : 10 : 25 w/w EVA/EGMA/WF composites. The observations were similar to those discussed previously.

Tensile testing

Figure 6 shows the modulus of uncompatibilized EVA–WF composites as function of WF content for different WF particle sizes. Generally, the modulus increased with increasing WF content. In a previous study, Ismail et al.[14] studied the physicomechanical properties of oil palm wood-flour-filled natural rubber composites, and they reported increased modulus and hardness with oil palm wood flour loading. Sedlackova et al.[12] studied EMAA as an effective compatibilizer of LDPE–WF composites and reported that the modulus increased gradually with increasing content of WF. Bledzki and Faruk[15] and Salemane and Luyt[9] studied polypropylene (PP)–WF composites and reported that the modulus of the PP–WF composite increased with increasing WF content. Balasuriya et al.[4] studied the mechanical properties of wood flake–polyethylene (PE) composites and reported that the modulus increased with increasing wood flake content. The increase in modulus is primarily influenced by the amount of filler loading, although the maximum values are dependent on the processing methods and flow behavior of the matrix agent.

We found that WF particle size had an influence on the modulus of the composite. As Figure 6 shows, the modulus decreased with increasing particle size. This finding was also reported by Ismail et al.[14] This was probably because composites made from small-particle-sized fillers show better filler dispersion and filler–matrix interaction than composites made from large particles. Interaction and interfacial adhesion is normally stronger for small particles than for larger ones.

The presence of 10% EGMA in the composites gave rise to much higher moduli than was observed for the uncompatibilized composites (Fig. 7). Similar results have also been obtained by other researchers. Elvy et al.[16] reported that the addition of alkoxysilane coupling agents modified the interface between dissimilar materials, such as glass fibers and thermoplastics or thermosetting resins, and, therefore, increased their tensile properties. Salemane and Luyt[9] reported that the use of a compatibilizer improved adhesion and, thus, enhanced the tensile properties of PP–WF composites. In their case, the composite properties changed with increasing maleated PP content. This improved filler–matrix interfacial adhesion was possibly caused by an esterification reaction between the hydroxyl groups of the cellulose filler and the anhydride functionalities of maleated PP. This interaction overcame the incompatibility problem and increased the tensile and flexural strength of the natural filler–polymer composites. Malunka et al.[10] reported that increasing sisal content and crosslinking and grafting gave rise to increased values of

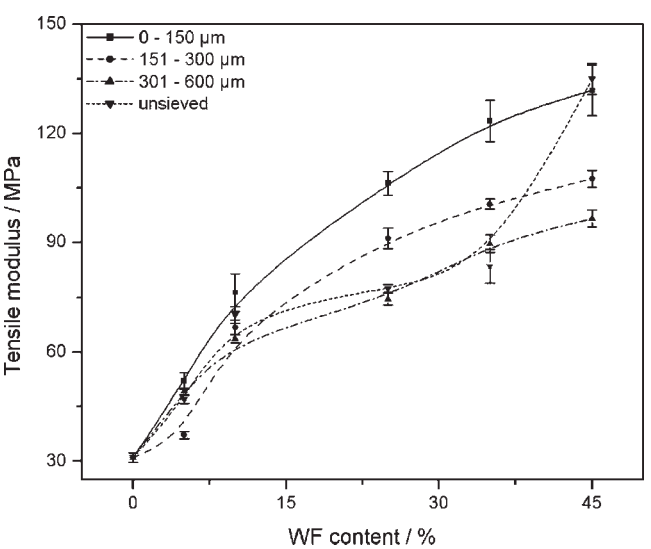

Figure 6 Tensile modulus as a function of WF content for samples containing different WF sizes in uncompatibilized composites.

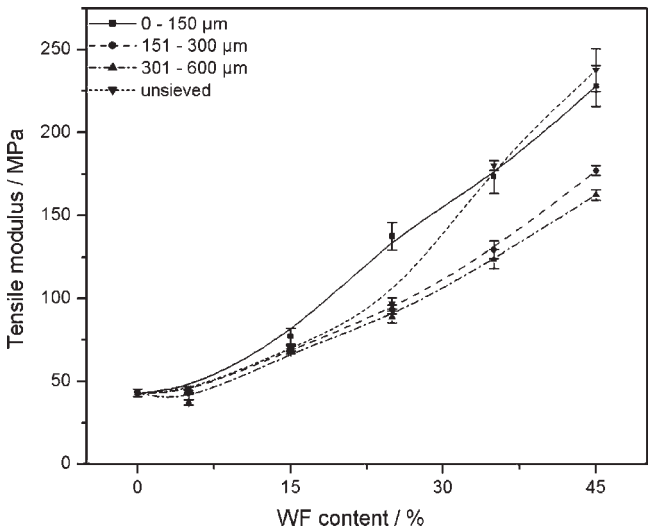

Figure 7 Tensile modulus as function of WF content for samples containing different WF sizes in 10% EGMA compatibilized composites.

Young's modulus. In our case, there was grafting between EGMA and WF,[17] which improved the wettability of WF and increased the interaction between WF and the EVA/EGMA matrix. However, there was still a decrease in tensile modulus with increasing WF particle size.

Figure 8 shows the stress at break curves of uncompatibilized EVA–WF composites. For all WF particle sizes, there was a continuous decrease in stress at break with increasing WF content, which was due to the weak interaction between WF and EVA. This was because of the hydrophobic and the hydrophilic natures of EVA and WF, respectively, as reported by Lee et al.[18] The inability of the filler to support stresses transferred from the polymer matrix increased with increasing filler loading. In the presence of WF, chain movement in EVA was restricted, and thus, its stress-handling capacity was considerably reduced.[2] Georgopoulos et al.[7] studied thermoplastic polymers reinforced with fibrous agricultural residue, and they reported a significant decrease in tensile stress when the polymer matrix was filled with natural fillers. The tensile strength also decreased with increasing particle size. The reason behind this was probably improved dispersion and filler–matrix interaction, which are normally observed for smaller particles.[14] Similar findings were reported by Biggs[19] and Fuad et al.[20] The unsieved WF composites had higher values of stress at break than the 151–300 and 301–600 µm WF composites. This confirmed that the unsieved WF consisted of mainly particles smaller than 150 µm. This was also clear from the water absorption results, which are discussed later.

The effect of the WF particle size and content on the stress at break behavior of the 10% EGMA compatibilized composites is shown in Figure 9. The 90 : 10 w/w EVA/EGMA blend had a lower stress at break value than pure EVA. The presence of 5% WF caused a reduction in the stress at break. However, an increase in WF content caused an increase in the stress at break of the composites. The reason was that an increase in WF content meant an increase in OH groups that reacted with EGMA, and the EGMA–WF grafted product interacted better with EVA, thus increasing the stress at break of the com-

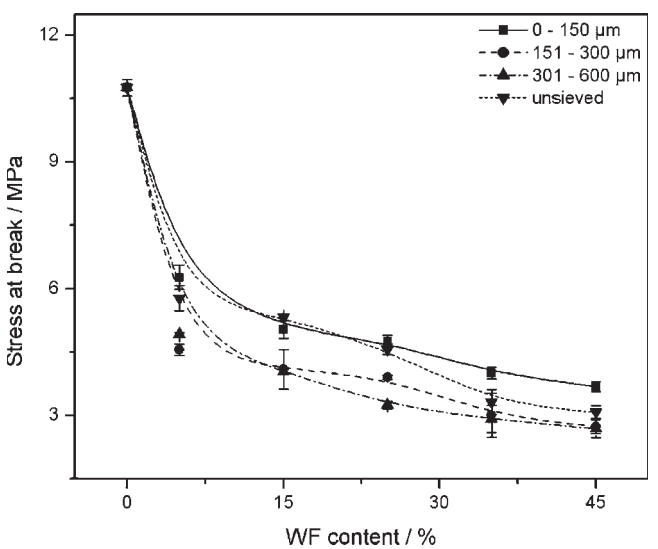

Figure 8 Stress at break as function of WF content for samples containing different WF sizes in the EVA–WF composites.

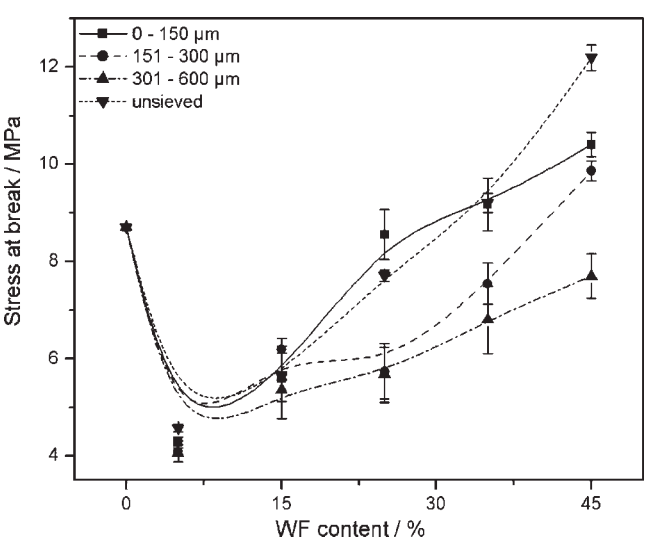

Figure 9 Stress at break as function of WF content for samples containing different WF sizes in 10% EGMA compatibilized composites.

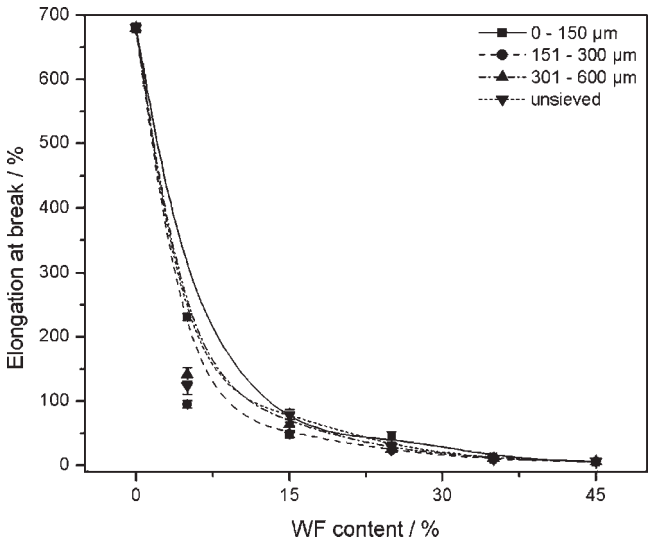

Figure 10 Elongation at break as function of WF content for samples containing different WF sizes in the EVA–WF composites.

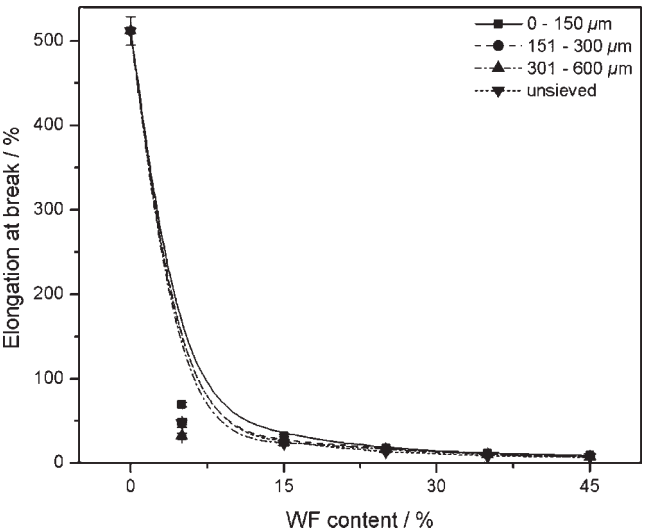

Figure 11 Elongation at break as function of WF content for samples containing different WF sizes in the 10% EGMA compatibilized composites.

posites. In this case, the smaller particle composites also showed higher tensile strengths.

The elongation at break curves of the uncompatibilized composites are shown in Figure 10. Pure EVA had the highest elongation (680%). The presence of WF in EVA led to a considerable decrease in the elongation at break values. This was the result of a restriction in the chain movement in EVA. As more WF was present, the stiffness and the brittleness of the composites increased. Georgopoulos et al.[7] reported a decrease in elongation at break; the composite seemed to lose most of its flexibility, even at low filler loadings. In this case, smaller WF particles had a less pronounced influence on the elongation at break of the samples, especially at filler contents of 15% and lower. The reason for this was probably that below 15%, there was a better dispersion of the small particles because the high EVA content reduced filler–filler interactions, and thus, the sample could be elongated to a higher value. However, at higher filler contents, the degree of filler–filler interaction became more prominent, even in the case of smaller particle composites, and as a result, a reduction in the elongation at break was seen. Balasuriya et al.[4] reported that the ultimate elongation values at yield or break (no yield was observed for composites containing more than 30 wt % WF) for PE–WF composites showed that ductility severely suffered from an increase in WF content. However, there was no significant difference in the elongation at break between different types of WF composites.

Figure 11 shows the elongation at break as function of WF content for the 10% EGMA compatibilized EVA–WF composites. The 90 : 10 w/w EVA/EGMA blend showed a lower elongation at break than pure EVA. This was because EGMA had a lower elongation at break than pure EVA. As in the uncompatibilized composites, there was also a strong decrease in the elongation at break for the WF-containing samples.

TGA

The TGA curves of the uncompatibilized composites are shown in Figure 12 for the composites containing particles smaller than 150 μm. The WF curve shows one degradation step with an onset temperature

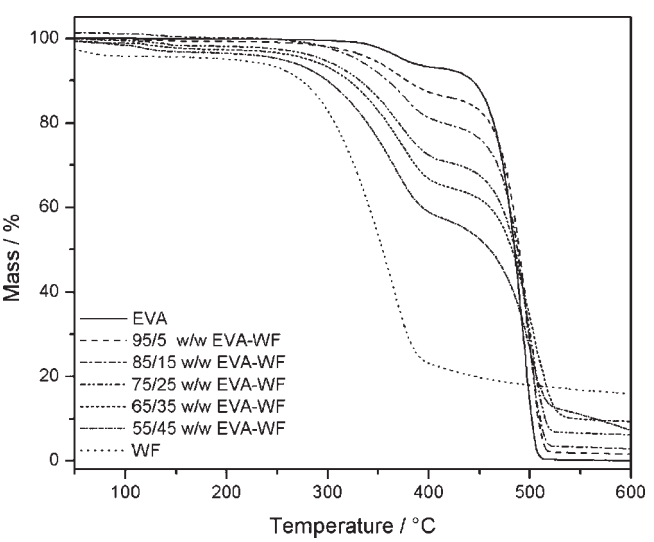

Figure 12 TGA curves of pure EVA, WF, and the EVA–WF composites (<150 μm).

around 200°C. EVA is characterized by two degradation steps. The first, related to the removal of acetate groups, starts at about 331°C. The second, due to the degradation of the PE backbone in EVA, occurs at about 460°C.[21,22] The EVA–WF composites also showed two degradation steps. The first degradation step was attributed to a combination of the decomposition of WF and the first step of the degradation of EVA, whereas the second step was attributed to the degradation of the EVA backbone. The onset temperatures of this step were higher than the observed onset temperature for pure WF. The onset temperatures of the first degradation step of the composites decreased with increasing WF content. The reason for this was probably that at low WF contents, the heat was mainly conducted by the EVA matrix, and as a result, the vinyl acetate scission started before the degradation of cellulose. At higher WF contents, the heat energy reached the WF particles much earlier, causing the WF particles to start degrading before EVA.

The effect of WF particle size on the degradation of the 75 : 25 w/w EVA/WF composites is shown in Figure 13. All sieved WF composites degraded in a similar way, regardless of the particle size used. WF particle size, therefore, did not seem to substantially influence the degradation behavior of EVA–WF composites.

The effect of particle size on the degradation of the 65 : 10 : 25 w/w EVA/EGMA/WF composites is shown in Figure 14. The first and second degradation steps occurred at the same temperatures, regardless of WF particle size. It is clear that when 10% EGMA was used, there was an insignificant difference in the degradation behavior of the composites, regardless of the particle size used. This shows that 10% EGMA effectively promoted interfacial bonding in the composites, even when unsieved particles were used.

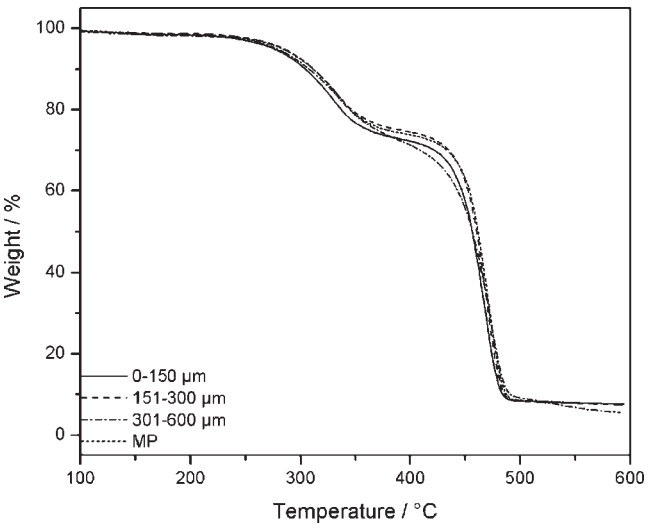

Figure 14 Effect of WF particle size on the degradation of the 65 : 10 : 25 w/w EVA/EGMA/WF composites.

Water absorption

Figure 15 shows the water absorption curves for the uncompatibilized composites containing 0–150 µm WF. Pure EVA absorbed water insignificantly, which was because of its hydrophobic nature and the fact that polymers' water absorption occurs only at the surfaces.[23] The presence of WF gave rise to an increase in water absorption. This was because WF is hydrophilic in nature; increasing amounts of WF corresponded to an increase in the number of OH groups and, thus, an increase in water absorption.

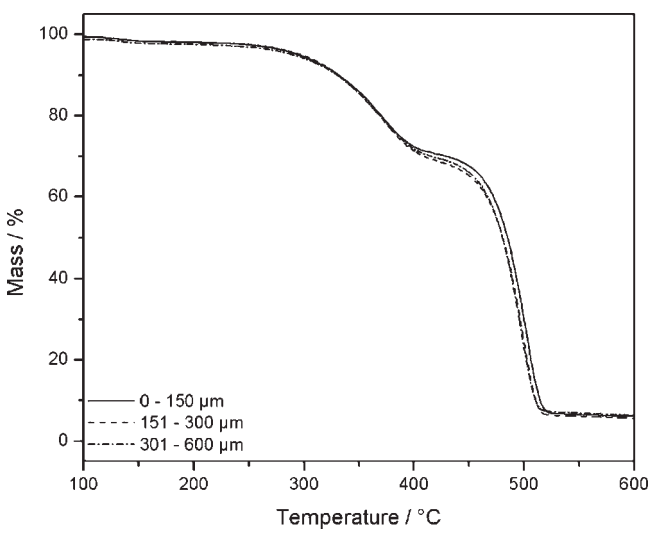

Figure 13 Effect of WF particle size on the degradation of the 75 : 25 w/w EVA/WF composites.

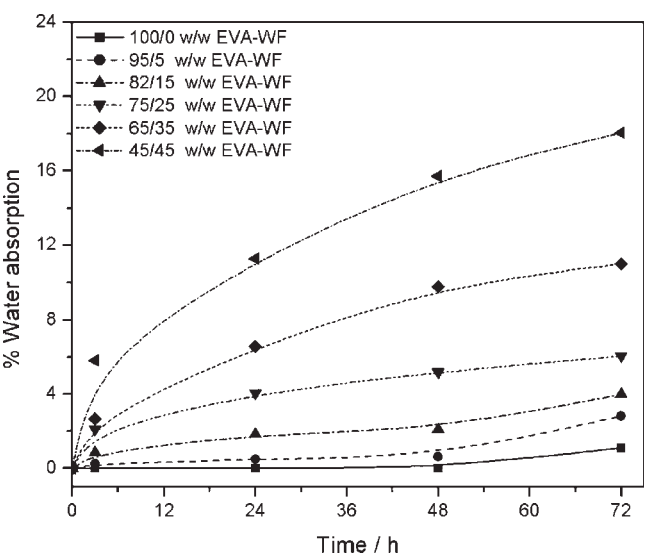

Figure 15 Effect of WF content on the water absorption of the uncompatibilized composites (<150 µm of WF).

The effect of filler particle size on the water absorption of composites at 25% filler loading is shown in Figure 16. Water absorption was higher in composites with smaller particle sizes. This was because smaller particles normally have larger surface areas and a higher exposure of OH groups from the cellulose, which would absorb more water. Ichazo et al.[23] studied water absorption of PP–WF composites and reported that water absorption was always high in larger particle size composites; they mentioned this to be a contradiction, as large surface areas were expected for small particles, and consequently, a higher availability of OH groups was expected. The reason given for their observation was the agglomeration of small particles.

The effect of particle size on the 10% EGMA compatibilized composites is shown in Figure 17. As in the previous case, the water absorption was the largest for the composites containing smaller WF particles. The grafting between EGMA and WF,[17] therefore, seemed to have little influence on the observed trend.

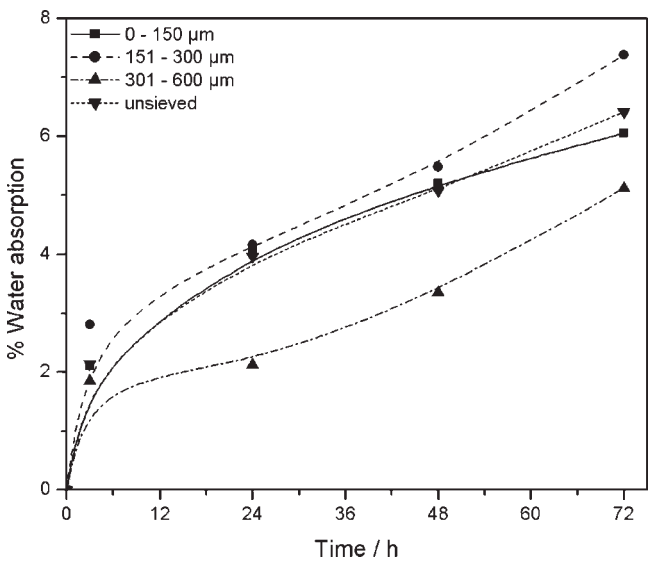

Figure 16 Effect of WF particle size on the water absorption of uncompatibilized composites at 25% WF loading.

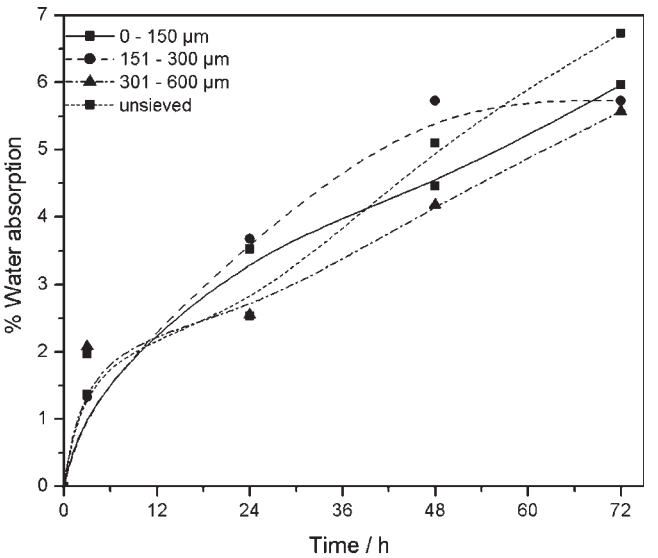

Figure 17 Effect of WF particle size on the water absorption of the 10% EGMA compatibilized composites at 25% WF loading.

CONCLUSIONS

Smaller WF particles showed better bonding to the matrix than larger particles, both in the presence and absence of EGMA. For both compatibilized and uncompatibilized composites, WF particle size did influence the crystallization behavior (as observed from the DSC results) of the EVA and EVA/EGMA matrices, but this influence showed no trend. In general, there was an increase in the tensile modulus with increasing WF content; the compatibilized composites had a higher modulus than the uncompatibilized ones. In both cases, composites containing smaller sized fillers had higher modulus values than those containing larger sized fillers. For uncompatibilized composites, the tensile strength decreased with increasing WF content, whereas for compatibilized composites, the tensile strength initially decreased but increased for composites containing more than 5% WF. Because of better dispersion and filler–matrix interaction, small-WF-particle-containing composites had higher tensile strengths than larger WF particle containing composites, both in the presence and absence of EGMA. For all of the samples, the elongation at break substantially decreased when WF was present. For both compatibilized and uncompatibilized composites, the initial degradation temperature depended on the amount of WF in the sample. WF particle size did not seem to have much influence on the degradation behavior of the composites. Water absorption by the composites seemed to be higher in smaller particle size composites because smaller particles had larger surface areas and, consequently, a higher exposure of OH groups. This was observed for both compatibilized and uncompatibilized composites.

References

1. Selke, E. S.; Wichman, I. Compos A 2004, 35, 321.
2. Ismail, H.; Jaffri, R. M. Polym Test 1999, 18, 381.
3. Tserkia, V.; Zafeiropoulos, N. E.; Simon, F.; Panayiotou, C. Compos A 2005, 36, 1110.
4. Balasuriya, P. W.; Ye, L.; Mai, Y. W. Compos A 2001, 32, 619.
5. Oksman, K.; Lindberg, H.; Holmgren, A. J Appl Polym Sci 1998, 68, 1845.

6. Maldas, D.; Kokta, B. V.; Raj, R. G.; Daneault, C. Polymer 1988, 29, 1255.
7. Georgopoulos, S. T.; Tarantili, P. A.; Avgerinos, E.; Andreopoulos, A. G.; Koukios, A. G. Polym Degrad Stab 2005, 90, 303.
8. Gassan, J.; Gutowski, V. S. Comp Sci Technol 2000, 60, 2857.
9. Salemane, M. G.; Luyt, A. S. J Appl Polym Sci 2006, 100, 4173.
10. Malunka, M. E.; Luyt, A. S.; Krump, H. J Appl Polym Sci 2006, 100, 1607.
11. Liao, B.; Huang, Y.; Cong, G. J Appl Polym Sci 1997, 66, 1561.
12. Sedlackova, M.; Lacik, I.; Chodak, I. Macromol Symp 2001, 170, 157.
13. Zaini, M. J.; Fuad, M. Y. A.; Ismail, Z.; Mansor, M. S. Polym Int 1996, 40, 51.
14. Ismail, H.; Rozman, H. D.; Jaffri, R. M.; Ishak, Z. A. M. Eur Polym J 1997, 33, 1627.
15. Bledzki, A.; Faruk, O. Comp Sci Technol 2004, 64, 693.
16. Elvy, S. B.; Dennis, G. R.; Teck, L. J Mater Process Technol 1995, 48, 365.
17. Dikobe, D. G.; Luyt, A. S. J Appl Polym Sci, to appear.
18. Lee, S. M.; Cho, D.; Park, W. H.; Lee, S. G.; Han, S. O.; Drzal, L. T. Comp Sci Technol 2005, 65, 647.
19. Biggs, D. M. Polym Comp 1987, 8, 115.
20. Fuad, M. Y. A.; Ismail, Z.; Ishak, Z. A. M.; Omar, A. K. Eur Polym J 1995, 31, 8.
21. Zanetti, M.; Camino, G.; Thomann, R.; Mulhaupt, R. Polymer 2001, 42, 4501.
22. Jansen, P.; Soares, B. G. Polym Degrad Stab 1996, 52, 95.
23. Ichazo, M. N.; Albano, C.; Gonzalez, J.; Perera, R.; Candal, M. V. Comp Struct 2001, 54, 201.